Probing cell type–specific functions of G_i in vivo identifies GPCR regulators of insulin secretion

Jean B. Regard, … , Matthias Hebrok, Shaun R. Coughlin

Research Article   Technical Advance   Cardiology

The in vivo roles of the hundreds of mammalian G protein–coupled receptors (GPCRs) are incompletely understood. To explore these roles, we generated mice expressing the S1 subunit of pertussis toxin, a known inhibitor of $G_{i/o}$ signaling, under the control of the *ROSA26* locus in a Cre recombinase–dependent manner ($ROSA26^{PTX}$). Crossing $ROSA26^{PTX}$ mice to mice expressing Cre in pancreatic β cells produced offspring with constitutive hyperinsulinemia, increased insulin secretion in response to glucose, and resistance to diet-induced hyperglycemia. This phenotype underscored the known importance of $G_{i/o}$ and hence of GPCRs for regulating insulin secretion. Accordingly, we quantified mRNA for each of the approximately 373 nonodorant GPCRs in mouse to identify receptors highly expressed in islets and examined the role of several. We report that 3-iodothyronamine, a thyroid hormone metabolite, could negatively and positively regulate insulin secretion via the G_i-coupled α_{2A}-adrenergic receptor and the G_s-coupled receptor Taar1, respectively, and protease-activated receptor–2 could negatively regulate insulin secretion and may contribute to physiological regulation of glucose metabolism. The $ROSA26^{PTX}$ system used in this study represents a new genetic tool to achieve tissue-specific signaling pathway modulation in vivo that can be applied to investigate the role of $G_{i/o}$-coupled GPCRs in multiple cell types and processes.

Find the latest version:

Probing cell type–specific functions of G_i in vivo identifies GPCR regulators of insulin secretion

Jean B. Regard,[1] Hiroshi Kataoka,[1] David A. Cano,[2] Eric Camerer,[1] Liya Yin,[1] Yao-Wu Zheng,[1] Thomas S. Scanlan,[1,3] Matthias Hebrok,[2] and Shaun R. Coughlin[1,2,3,4]

[1]Cardiovascular Research Institute, [2]Diabetes Center, [3]Department of Cellular and Molecular Pharmacology, and [4]Department of Medicine, UCSF School of Medicine, San Francisco, California, USA.

The in vivo roles of the hundreds of mammalian G protein–coupled receptors (GPCRs) are incompletely understood. To explore these roles, we generated mice expressing the S1 subunit of pertussis toxin, a known inhibitor of $G_{i/o}$ signaling, under the control of the *ROSA26* locus in a Cre recombinase–dependent manner (*ROSA26^{PTX}*). Crossing *ROSA26^{PTX}* mice to mice expressing Cre in pancreatic β cells produced offspring with constitutive hyperinsulinemia, increased insulin secretion in response to glucose, and resistance to diet-induced hyperglycemia. This phenotype underscored the known importance of $G_{i/o}$ and hence of GPCRs for regulating insulin secretion. Accordingly, we quantified mRNA for each of the approximately 373 nonodorant GPCRs in mouse to identify receptors highly expressed in islets and examined the role of several. We report that 3-iodothyronamine, a thyroid hormone metabolite, could negatively and positively regulate insulin secretion via the G_i-coupled α_{2A}-adrenergic receptor and the G_s-coupled receptor Taar1, respectively, and protease-activated receptor–2 could negatively regulate insulin secretion and may contribute to physiological regulation of glucose metabolism. The *ROSA26^{PTX}* system used in this study represents a new genetic tool to achieve tissue-specific signaling pathway modulation in vivo that can be applied to investigate the role of $G_{i/o}$-coupled GPCRs in multiple cell types and processes.

Introduction

G protein–coupled receptors (GPCRs) regulate myriad physiological and disease processes and have been a rich source of targets for pharmaceuticals (1). About 40% of the estimated 370–400 non-odorant GPCRs in mice and humans remain orphans (2), and new roles for receptors with known ligands are regularly uncovered. Despite the number and diversity of GPCRs, their ligands, and the processes they govern, GPCRs couple to intracellular signaling pathways through only 4 relatively small families of G proteins: G_s, G_i, G_q, and $G_{12/13}$. Thus, one strategy to probe for necessary roles of GPCR signaling in vivo has been to ablate the function of such G proteins in mice (3–6). G_i function has been difficult to fully ablate by standard knockout technology because of partial redundancy among G_i family members, particularly $G\alpha_{i1}$, $G\alpha_{i2}$, $G\alpha_{i3}$, $G\alpha_o$, and $G\alpha_z$.

We report the development of a system to probe the function of G_i family members and the receptors that regulate them in vivo and the use of this system to uncover potential regulators of insulin secretion. We generated a mouse line in which the catalytic S1 subunit of *Bordetella pertussis* toxin (PTX) was expressed in a cell type–specific Cre recombinase–dependent manner. PTX ADP-ribosylates and uncouples all G_i family members except G_z from upstream GPCRs (7) and hence largely circumvents the redundancy noted above. To identify candidate GPCRs that might explain new phenotypes

uncovered by cell type–specific inhibition of $G_{i/o}$, we also generated TaqMan primer/probe sets for quantitative RT-PCR (qRT-PCR) of all nonodorant GPCRs annotated in the mouse genome.

We chose to first characterize this system in pancreatic β cells for several reasons. First, acute dosing of rodents with pertussis holotoxin has long been known to increase plasma insulin, and treatment of cultured islets and β cell lines with pertussis enhances insulin secretion (8–11). This gain-of-function phenotype in β cells offered an opportunity to determine whether long-term expression of PTX in vivo might negatively affect the differentiation, development, or health of cells and tissues and whether it could indeed produce appropriate cell type–specific, cell-autonomous, and signaling pathway–specific phenotypes. Second, in contrast to classic pharmacological studies, expression of PTX in β cells would probe the relative importance of GPCR signaling via $G_{i/o}$ among the many regulators of insulin secretion in vivo over relatively long periods of time. Insulin resistance with insulin secretion that is chronically insufficient for normal glucose homeostasis plays a key role in metabolic syndrome and type 2 diabetes mellitus, and a more complete understanding of how insulin secretion is modulated by GPCR signaling might provide new strategies for treating these epidemic disorders. Third, regulation of insulin secretion is well studied, and we expected that having a set of GPCRs known to regulate insulin secretion might be instructive for prioritizing new candidate GPCRs derived from expression profiling.

Here we show that PTX expression in β cells produced hyper-insulinemic mice with high levels of glucose-stimulated insulin release. This result together with improved glucose tolerance and resistance to diet-induced diabetes in these mice underscored the importance of β cell $G_{i/o}$, and hence of GPCR signaling, in the regulation of glucose metabolism both moment to moment and over
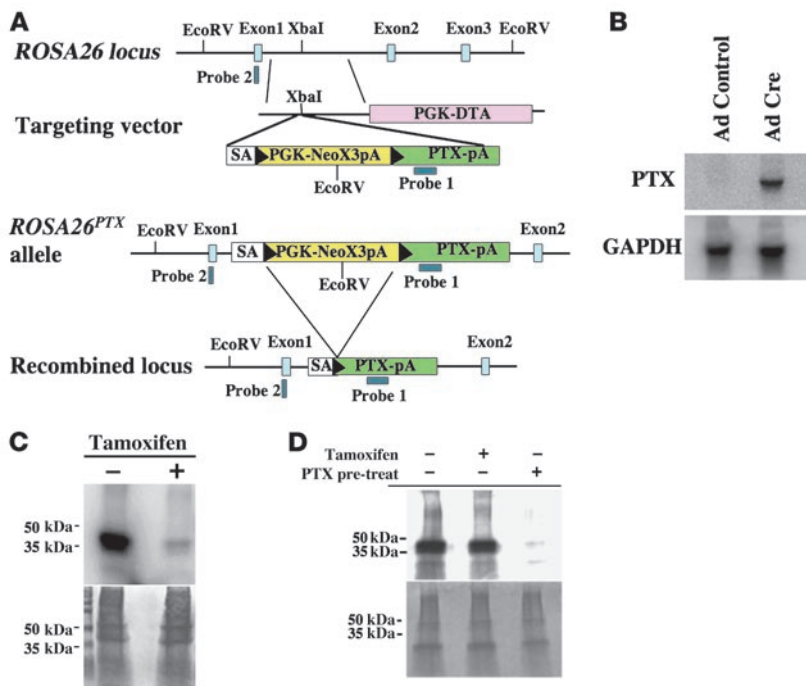

Figure 1
Generation and characterization of the conditional *ROSA26^PTX* allele. (**A**) Diagram of the wild-type *ROSA26* locus, the *ROSA26^PTX* targeting vector, the *ROSA26*^PTX allele, and Cre-recombined locus. Black arrowheads represent LoxP sites. (**B**) Cre-dependent expression of PTX S1 mRNA. RNA from endothelial cells that were isolated from *ROSA26^PTX* mice and then infected with Cre- or GFP-expressing (control) adenovirus was analyzed by Northern blot. Blots were hybridized with probe for PTX S1 and for GAPDH mRNA to assess loading. (**C**) Cre-dependent ADP-ribosylation of G$\alpha_{i/o}$. Fibroblasts from *ROSA26^PTX* mouse embryos carrying a CMV-IE-ER-Cre transgene were incubated with or without 1 μM 4-hydroxy-tamoxifen for 4 days to induce Cre expression, *ROSA26^PTX* recombination, and expression of PTX S1. Membranes from these cells were incubated with the ADP-ribose donor [^{32}P]NAD and exogenous pertussis toxin, then analyzed by SDS-PAGE and autoradiography (upper panel) or stained for protein loading (lower panel). Note the absence of G$\alpha_{i/o}$ available for in vitro labeling in membranes from tamoxifen-induced cells, indicating that ADP-ribosylation of G$\alpha_{i/o}$ had already occurred in vivo. (**D**) Cell-autonomous function of *ROSA26^PTX*. Mouse thymocytes were cocultured with Cre-expressing *ROSA^PTX* mouse embryonic fibroblasts (MEFs; as in Figure 1C). Where indicated (+pre-treat), thymocytes were treated with pertussis holotoxin (50 ng/ml). After 8 hours of coculture, thymocytes were isolated, and their membrane fractions were assayed for G$\alpha_{i/o}$ available for in vitro ADP-ribosylation as in Figure 1C. Note that coculture of thymocytes with PTX S1–expressing MEFs did not cause detectable loss of ADP-ribosylatable G$\alpha_{i/o}$, but addition of exogenous holotoxin did.

expressed upon excision of a floxed silencer cassette by Cre recombinase (*ROSA26^PTX* allele; Figure 1A) (12). Southern blotting confirmed correct targeting as well as the expected Cre-dependent excision of the silencer (Supplemental Figure 1; supplemental material available online with this article; doi:10.1172/JCI32994DS1). In the absence of a Cre transgene, *ROSA26^PTX/+* and *ROSA26^PTX/PTX* mice were born at the expected Mendelian rate and were indistinguishable in appearance from wild-type littermates. In cells isolated from *ROSA26^PTX/PTX* mice, PTX mRNA was detected in the presence but not in the absence of Cre expression (Figure 1B). In *ROSA26^PTX* cells that expressed a tamoxifen-dependent Cre (13), tamoxifen treatment led to nearly complete ADP-ribosylation of G$\alpha_{i/o}$, as measured by a decrease in G$\alpha_{i/o}$ available to accept radiolabeled ADP-ribose upon addition of exogenous pertussis toxin to membranes prepared from these cultures (Figure 1C). The low level of residual G$\alpha_{i/o}$ ADP-ribosylation seen in these preparations may have been due to the presence of a small fraction of cells that did not undergo Cre-mediated excision.

Expression of the S1 catalytic subunit of PTX in the absence of the S2–5 subunits of PTX holotoxin should cause cell-autonomous effects, as the S2–5 subunits are required to deliver the S1 catalytic subunit from the extracellular environment to the cytoplasm (14). To test this prediction, Cre recombinase–expressing *ROSA26^PTX/PTX* mouse embryonic fibroblasts (MEFs) were cocultured in direct contact with naive mouse thymocytes. Thymocytes were later isolated and the ADP-ribosylation state of G$\alpha_{i/o}$ analyzed. ADP-ribosylation of G$\alpha_{i/o}$ in the MEFs themselves was virtually complete under these conditions (Figure 1C), but ADP-ribosylation of G$\alpha_{i/o}$ in the cocultured thymocytes was undetectable (Figure 1D). Nearly complete ADP-ribosylation of G$\alpha_{i/o}$ did occur when thymocytes were incubated with PTX holotoxin (Figure 1D). These data suggested that the S1 subunit of PTX expressed from the *ROSA26* locus indeed acted within the cells in which it was expressed and not in neighboring cells, which in turn predicted that crosses of *ROSA26^PTX* mice with mice carrying lineage-specific Cre transgenes would yield cell autonomous, cell type–specific phenotypes.

Expression of PTX in β cells leads to hyperinsulinemia and hypoglycemia. We crossed *ROSA26^PTX/PTX* mice with mice carrying the rat insulin promoter (RIP) Cre transgene, which is expressed in β cells of pancreatic islets (15, 16) and in a small number of neurons in the hypothalamus (17, 18). Crosses of male mice hemizygous for the RIP-Cre transgene (RIP-Cre Tg$^{+/o}$) to *ROSA26^PTX/PTX* females produced RIP-Cre Tg$^{+/o}$:*ROSA26^PTX/+* offspring at the expected Mendelian ratio. These mice, hereafter referred to as RIP-PTX mice, were normal in appearance and showed pancreatic islet size, number, histological appearance, and cellular composition similar to those of wild-type and control mice (Figure 2, A and B, and Supplemental Figure 2). Islet morphology remained normal in RIP-PTX mice even

time. Accordingly, we measured mRNA levels for all nonodorant mouse GPCRs in isolated pancreatic islets and investigated several highly expressed candidates. Our results point to new potential regulators of insulin secretion. Our results also show that chronic lineage-specific expression of pertussis toxin S1 subunit in mice can yield an appropriate cell-autonomous and signaling pathway–specific phenotype. This system will be useful for uncovering in vivo roles of G$_{i/o}$-coupled GPCRs in any cell type or lineage for which a Cre transgene is available.

Results

Generation and characterization of the ROSA26^PTX allele. We generated a mouse in which a cDNA encoding the S1 catalytic subunit of PTX was inserted into the *ROSA26* locus such that PTX S1 would be
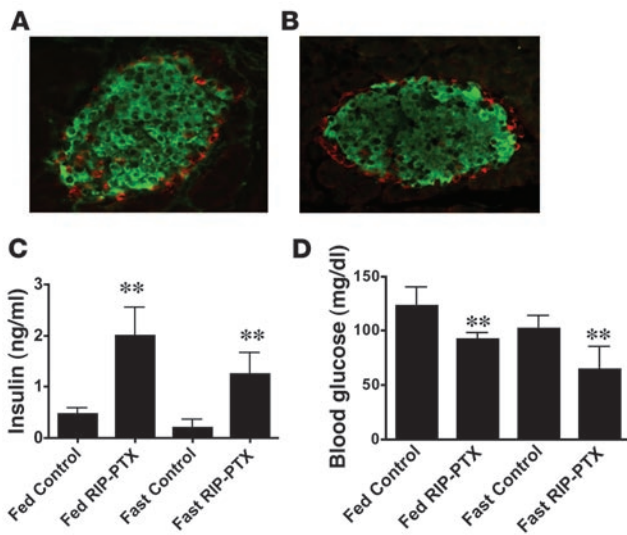
Figure 2
Anatomically normal islets, hyperinsulinemia, and hypoglycemia in RIP-PTX mice. (**A** and **B**) Immunofluorescent staining of pancreas sections from control (**A**) and RIP-PTX (**B**) mice for insulin (green; β cells) and glucagon (red; α cells) (original magnification, ×20). Islet size, morphology, and cellular composition and number were unchanged in RIP-PTX mice. (**C**) Plasma insulin levels in 8- to 10-week-old RIP-PTX mice and littermate controls (n = 8–11; **P < 0.001); mice were fed ad libitum or fasted overnight as indicated. Plasma insulin levels were elevated in RIP-PTX under both fed and fasted conditions. (**D**) Blood glucose levels in RIP-PTX mice and littermate controls (n = 8–11; **P < 0.001). RIP-PTX mice were hypoglycemic under both fed and fasted conditions.

at 1.5 years of age, suggesting that chronic PTX expression does not adversely affect β cell health. In addition, given that the RIP-Cre transgene is first expressed at mid-gestation (16), PTX expression in β cells does not appear to disrupt normal islet development.

Despite having anatomically normal islets, RIP-PTX mice showed markedly dysregulated insulin secretion. Plasma insulin levels in RIP-PTX mice were 4- to 5-fold higher than in wild-type mice or Cre-negative $ROSA26^{PTX/+}$ littermate controls in both fed and fasted states (Figure 2C), and insulin mRNA levels were increased in pancreas from RIP-PTX mice compared with littermate controls (Supplemental Figure 3). Hyperinsulinemia was accompanied by relative hypoglycemia (Figure 2D). These data suggest that tonic $G_{i/o}$ stimulation plays an important role in regulating basal insulin production.
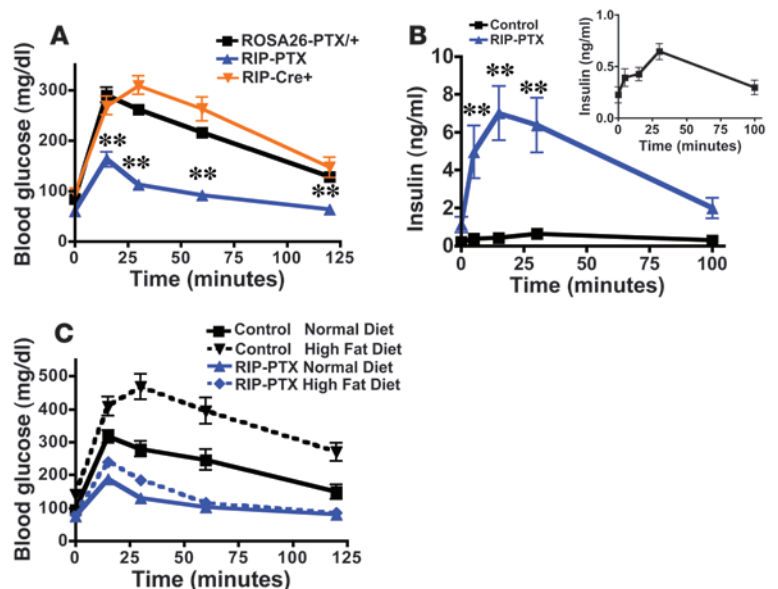
Compared with Cre-negative $ROSA26^{PTX/+}$ mice, RIP-PTX mice showed dramatically enhanced glucose clearance from plasma as assessed by i.p. glucose tolerance testing (IPGTT) (Figure 3A). Glucose clearance in RIP-Cre transgene–positive, $ROSA26^{+/+}$ con-
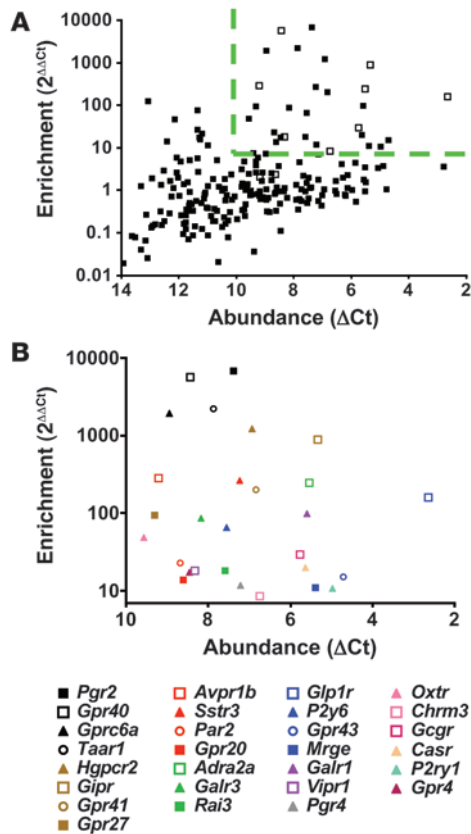
trol mice was, if anything, mildly impaired relative to that in Cre-negative $ROSA26^{PTX/+}$ mice (Figure 3A; see also Supplemental Figure 2), indicating that the RIP-Cre transgene and the $ROSA26^{PTX}$ allele were both required for the RIP-PTX phenotype. Crosses of $ROSA26^{PTX/PTX}$ mice with mice bearing a pancreatic and duodenal homeobox–1–Cre (PDX-Cre) transgene (19), which is expressed in β cells as well as other foregut cell types, yielded mice with a phenotype similar to that of RIP-PTX mice (Supplemental Figure 4). Thus, the hyperinsulinemia and hypoglycemia in RIP-PTX mice was almost certainly due to Cre-mediated recombination of the $ROSA26^{PTX}$ locus in β cells.

The marked blunting of elevations in blood glucose after i.p. glucose administration in RIP-PTX mice suggested that these mice might have exaggerated insulin secretion in response to glucose stimulation. Indeed, glucose administration triggered an approximately 6.5-fold increase in plasma insulin over the already elevated basal level in RIP-PTX mice compared with a 3-fold increase over basal in controls (Figure 3B and inset). Strikingly, the peak insulin

Figure 3
RIP-PTX mice show improved glucose tolerance and resistance to high-fat diet–induced hyperglycemia. (**A**) IPGTT in 8- to 10-week-old male RIP-PTX mice, littermate controls, and age-matched, background-matched RIP-cre mice. Glucose (2 mg/g) was administered i.p. at time 0, and plasma glucose was measured at the indicated time points. Note the lower glucose levels in RIP-PTX mice compared with controls (n = 9–10; **P < 0.0001). (**B**) GSIS. Glucose was administered at 3 mg/g i.p. to mice as in **A**, and plasma insulin levels were measured at the indicated times. Note the 6.5-fold increase over already elevated basal levels in RIP-PTX mice compared with a 3-fold increase in controls (inset) (n = 7–8; **P < 0.0001). (**C**) IPGTT in RIP-PTX mice and littermate controls fed a normal or high-fat diet for 30 weeks. RIP-PTX mice fed a high-fat diet had glucose levels significantly lower than controls on a high-fat diet (n = 8–11; P < 0.0001) and lower than controls on a normal diet (n = 8–10; P = 0.007).

level achieved after glucose administration to RIP-PTX mice was 15-fold higher than that achieved in controls (Figure 3B). In addition, after 30 weeks on a high-fat diet, control mice had elevated fasting blood glucose levels and impaired glucose tolerance compared with control mice maintained on normal diet for the same period. By contrast, fasting blood glucose levels and glucose tolerance remained within the normal range in RIP-PTX littermates maintained on a high-fat diet for the same period (Figure 3C).

Taken together, these results support an important role for $G_{i/o}$ signaling in β cells in moment-to-moment regulation of insulin secretion and in longer-term regulation of glucose homeostasis and the development of a diabetes-like state.

Expression profile of islet GPCRs by qRT-PCR. The importance of $G_{i/o}$ signaling for short- and long-term glucose homeostasis and the fact that the magnitude of hyperinsulinemia in RIP-PTX mice was substantially greater than that in mice lacking individual G_i-coupled receptors known to negatively modulate insulin release (20–22) prompted an effort to enumerate candidate GPCRs that might contribute to regulation of insulin secretion by β cells. Toward identifying GPCRs that are most highly and specifically expressed in pancreatic islets, we generated primer and probe sets for qRT-PCR of the 373 nonodorant GPCRs found in the mouse genome (23). GPCR expression levels were plotted as a function of abundance (level of each GPCR mRNA normalized to level of housekeeping gene mRNAs in the same islet preparation) and enrichment (abundance in islets relative to abundance in a mixed tissue sample). Receptors known to play an important role in regulating β cell insulin secretion (24–27) (Figure 4A, open squares) were among those expressed most highly and most specifically in islets. Indeed, among the 28 most highly and specifically expressed

receptors (Figure 4B and Table 1), 8 GPCRs are known to be physiologically important regulators islet function (Figure 4B, open squares). An additional 11 of these 28 GPCRs have ligands known to regulate insulin release (filled triangles), but a physiological role for these versus related receptors in β cell function has not been confirmed. Of the remaining 9 GPCRs, 5 are orphans (filled squares) and 4 have known ligands (open circles) not previously implicated in β cell function. Of these 4, trace amine receptor–1 (Taar1) (28, 29) was the most islet specific, and protease-activated receptor–2 (Par2; also known as F2rl1) was intriguing because its ability to sense trypsin-like proteases (30) suggested the possibility of an unexpected role for proteases in this system. These receptors were selected for further study.

3-Iodothyronamine is a novel regulator of insulin release. We confirmed that *Taar1* is expressed in mouse β cells by in situ hybridization for *Taar1* mRNA in pancreas sections (Supplemental Figure 5). Similarly, qRT-PCR analysis of mRNA isolated from 2 mouse β cell lines and from human islet preparations confirmed *Taar1* expression in those tissues (Supplemental Figure 6).

3-Iodothyronamine (T1AM), a thyroid hormone metabolite found in plasma and tissue extracts, was recently found to be an agonist for Taar1 (31). Administration of T1AM (50 mg/kg, i.p.) increased blood glucose and decreased insulin levels in wild-type and Cre-negative *ROSA26^(PTX/+)* mice. Blood glucose levels reached approximately 250% of basal levels 2 hours following T1AM administration and returned to basal by 8 hours (Figure 5A). At 2 hours following T1AM injection, blood insulin levels were decreased to approximately 40% of normal basal levels (Figure 5B), and administration of exogenous insulin at that time led to a rapid reversal of the elevated blood glucose levels (Supplemental Figure 7). Thus, peripheral tissues remained sensitive to insulin following T1AM treatment.

In addition to decreasing plasma insulin, T1AM administration caused an approximately 2-fold increase in plasma glucagon levels (Supplemental Figure 8). This is consistent with the T1AM-induced reduction in intra-islet insulin release and perhaps hyperglycemia itself promoting glucagon secretion by α cells (32). The relative importance of decreased insulin versus increased glucagon for the hyperglycemic effects of T1AM remains to be determined.

Importantly, T1AM had no effect on glucose and insulin levels in RIP-PTX mice (Figure 5, A and B). Moreover, T1AM inhibited glucose-stimulated insulin secretion (GSIS) in vitro in freshly isolated

Table 1
GPCRs abundant and highly enriched in mouse islets

Gene name	NCBI accession	Receptor name (alias)	Ligand	Effects on insulin secretion
Glp1r	NM_021332	Glucagon-like peptide (GLP) receptor 1 GLP	Increases	
Gpr41	NM_001033316	Free fatty acid receptor 3 (ffar3)	Short-chain fatty acids	???
Gpr40	NM_194057	FFA receptor 1 (ffar1)	Long-chain fatty acids	Increases
Adra2a	NM_007417	α_{2A} adrenergic	Epinephrine/norepinephrine	Decreases
Gipr	NM_001080815	Gastric inhibitory polypeptide (GIP) receptor	GIP	Increases
Pgr2	NM_181749	Pgr2 (Gpr142)	Unknown	???
Hgpcr2	NM_181751	Hgpcr2 (Gpr119)	Lysophospholipids	Increases
Galr1	NM_008082	Galanin receptor 1	Galanin	Decreases
Sstr3	NM_009218	Somatostatin receptor 3	Somatostatin	Decreases
Taar1	NM_053205	Trace amine associated receptor 1	3-Iodothyronamine	???
Gprc6a	NM_153071	Gprc6a	Basic amino acids?	Increases?
Gcgr	NM_008101	Glucagon receptor	Glucagon	Increases
Avpr1b	NM_011924	Vasopressin 1b receptor	Vasopressin	Increases
Casr	NM_013803	Extracellular calcium-sensing receptor	Calcium	Increases?
P2ry6	NM_183168	P2Y purinoceptor 6	UTP/UDP	Increases?
Galr3	NM_015738	Galanin receptor 3	Galanin	Decreases
Gpr27	NM_008158	Gpr27 (Sreb1)	Unknown	???
P2ry1	NM_008772	P2Y purinoceptor 1	ATP	Increases
Mrge	NM_175534	Mas-related GPCR e	Unknown	???
Rai3	NM_181444	Retinoic acid induced 3, Raig1, Gprc5a	Unknown	???
Oxtr	NM_001081147	Oxytocin receptor	Oxytocin	Increases
Par2	NM_007974	Protease-activated receptor 2 (f2rl1)	Serine proteases	???
Pgr4	NM_181748	Pgr4 (Gpr120)	Long-chain fatty acids	Increases
Vipr1	NM_011703	Vasoactive intestinal polypeptide (VIP) receptor 1	VIP	Increases
Gpr4	NM_175668	Gpr4	Sphingolipids, protons	Increases
Gpr20	NM_173365	Gpr20	Unknown	???
Gpr43	NM_146187	FFA receptor 2 (ffar2)	Short-chain fatty acids	???
Chrm3	NM_033269	M3 muscarinic acetylcholine receptor	Acetylcholine	Increases

Pancreatic islets were isolated from adult C57BL/6 mice, and quantification of GPCRs expressed was assessed by qRT-PCR. In 5 independent experiments, mRNAs for these receptors were consistently abundant and enriched in islets relative to mixed tissues.

mouse and human islets, and this effect of T1AM was blocked by pretreatment of islets with PTX (Figure 5, C and D). These results strongly suggest that T1AM activates a $G_{i/o}$-coupled receptor on β cells to inhibit insulin secretion. Is this receptor Taar1? In heterologous expression systems, Taar1 activation by T1AM has been reported to increase cytoplasmic cAMP levels (28, 29, 31), suggesting coupling to G_s, and we failed to detect coupling of Taar1 to G_i in a *Xenopus* oocyte expression system in which M2 muscarinic receptor coupling to G_i was readily detected (Supplemental Figure 9). This led us to explore the alternative hypothesis that T1AM activates $G_{i/o}$ and inhibits insulin secretion via a β cell GPCR other than Taar1. T1AM shares chemical features with catecholamines, the classical adrenergic receptor ligands (Figure 5E), and α_{2A} adrenergic receptor (Adra2a), which is $G_{i/o}$ coupled (33), was highly expressed in islets (Figure 4B). A screen performed by the National Institutes of Mental Health Psychoactive Drug Screening Program suggested that T1AM can bind to human Adra2a (personal communication from Bryan Roth, University of North Carolina, Chapel Hill, North Carolina, USA). Thus, Adra2a was a candidate for a $G_{i/o}$-coupled mediator of T1AM effects in β cells.

Membrane binding experiments demonstrated that T1AM bound to Adra2a with an affinity similar to or better than that of epinephrine (Figure 5F). Coadministration of the Adra2a antagonist yohimbine with T1AM inhibited T1AM's hyperglycemic effects (Supplemental Figure 10), and T1AM failed to cause

hyperglycemia in *Adra2a*-null mice (Figure 5G). Pretreatment of mice with 6-OH dopamine to ablate adrenergic neurons did not diminish T1AM-induced hyperglycemia (Supplemental Figure 11). These data strongly suggest that T1AM's inhibitory effect on insulin release in vivo is mediated by the Adra2a in β cells in a $G_{i/o}$-dependent manner.

What role if any does Taar1 play in β cell responses to T1AM? It is interesting to note that the relative expression levels of *Adra2a* and *Taar1* were reversed in the MIN6 insulinoma cell line versus normal mouse islets (*Taar1* mRNA was upregulated greater than 200-fold in MIN6 cells; Supplemental Figure 6), and exposure of MIN6 cells to T1AM resulted in increased rather than decreased insulin secretion (Supplemental Figure 12). This increase was further augmented by treatment with PTX or yohimbine (Supplemental Figure 12). These results are consistent with the notion that T1AM can stimulate insulin secretion via G_s-coupled Taar1 and inhibit it via G_i-coupled Adra2a. In MIN6 cells, in which *Taar1* expression is high relative to that of *Adra2a*, the Taar1 effect dominates. In β cells in vivo, in which *Adra2a* is more highly expressed than *Taar1* (Figure 4B), the Adra2a effect dominates. Consistent with this model, *Adra2a*-null mice became hypoglycemic after T1AM injection (Figure 5G), suggesting that the effect of Taar1 activation on insulin secretion became detectable in the absence of Adra2a function. Whether the striking upregulation of Taar1 with respect to Adra2a seen in MIN6 cells is ever recapitulated in vivo is unknown.
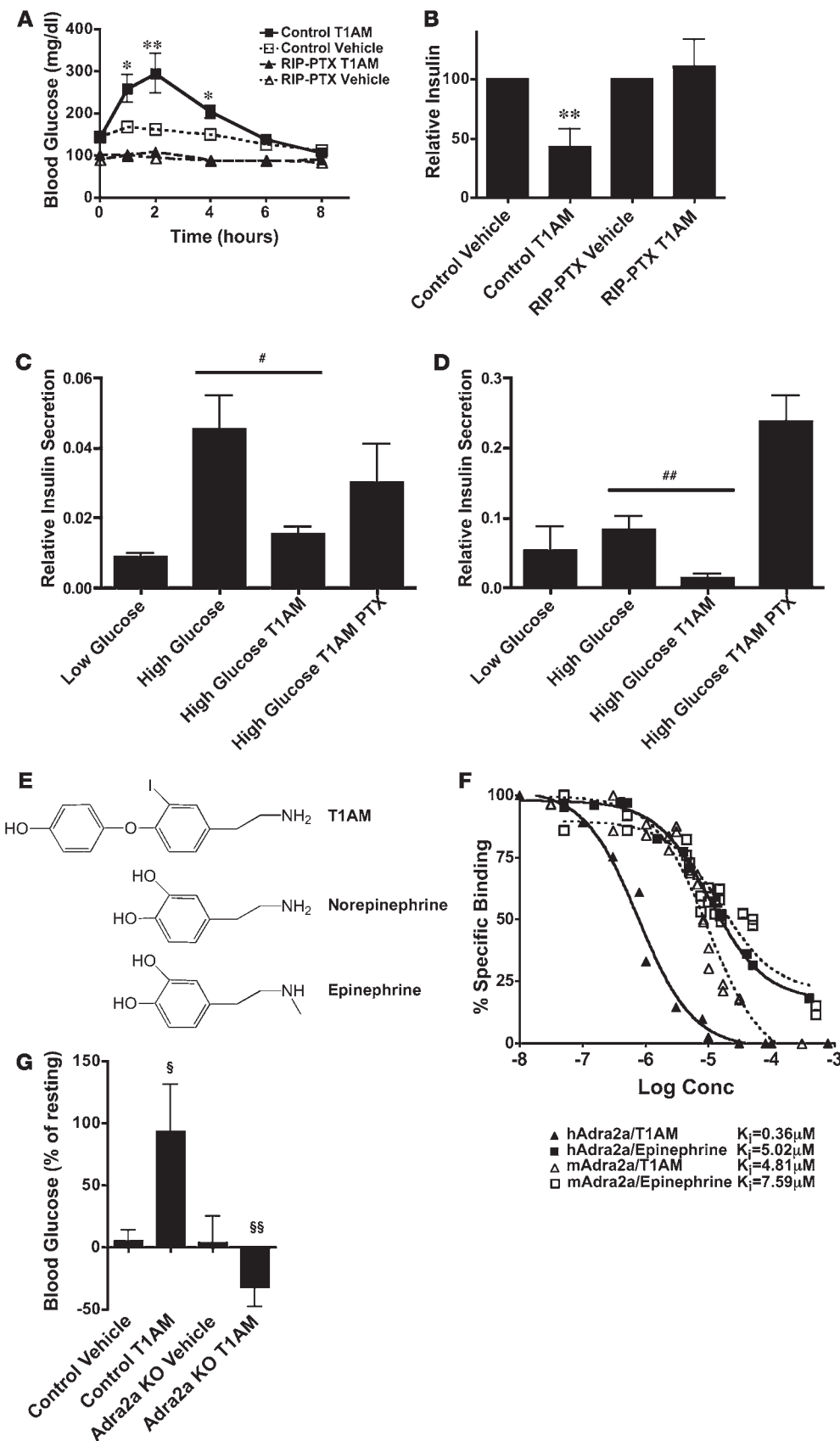
Figure 5

Administration of T1AM causes Adra2a- and G_i-dependent hyperglycemia and hypoinsulinemia. (**A**) Blood glucose levels following administration of T1AM (50 mg/kg, i.p.) or vehicle. T1AM induced hyperglycemia in wild-type ($n = 6$–7; *$P < 0.01$, **$P < 0.001$) but not in RIP-PTX mice. (**B**) Blood insulin levels 2 hours following vehicle or T1AM injection as in **A** relative to preinjection levels. Note the 60% decrease in insulin levels after T1AM in wild-type ($n = 6$; #$P < 0.005$) but not RIP-PTX mice. (**C** and **D**) The effects of T1AM on GSIS in isolated islets from mice (**C**) and humans (**D**). T1AM (10 μM) was capable of inhibiting GSIS in a PTX-sensitive manner in both species (PTX pretreatment 50 ng/ml for 16 hours). Data are presented as relative insulin secreted/total insulin (mean ± SEM; $n = 3$–4; ##$P < 0.05$). (**E**) Chemical similarity of T1AM and catecholamines. (**F**) Competition of T1AM and epinephrine for [^{3}H]RX821002 binding to membranes from Cos cells transfected with an expression vector for human or mouse Adra2a. Binding of [^{3}H]RX821002 was Adra2a transfection dependent. (**G**) Blood glucose levels 1 hour following T1AM administration to control mice and *Adra2a*-null mice. Note that control mice became hyperglycemic following T1AM administration ($n = 9$; §$P = 0.001$), but *Adra2a*-null mice became hypoglycemic ($n = 11$–12; §§$P = 0.003$).
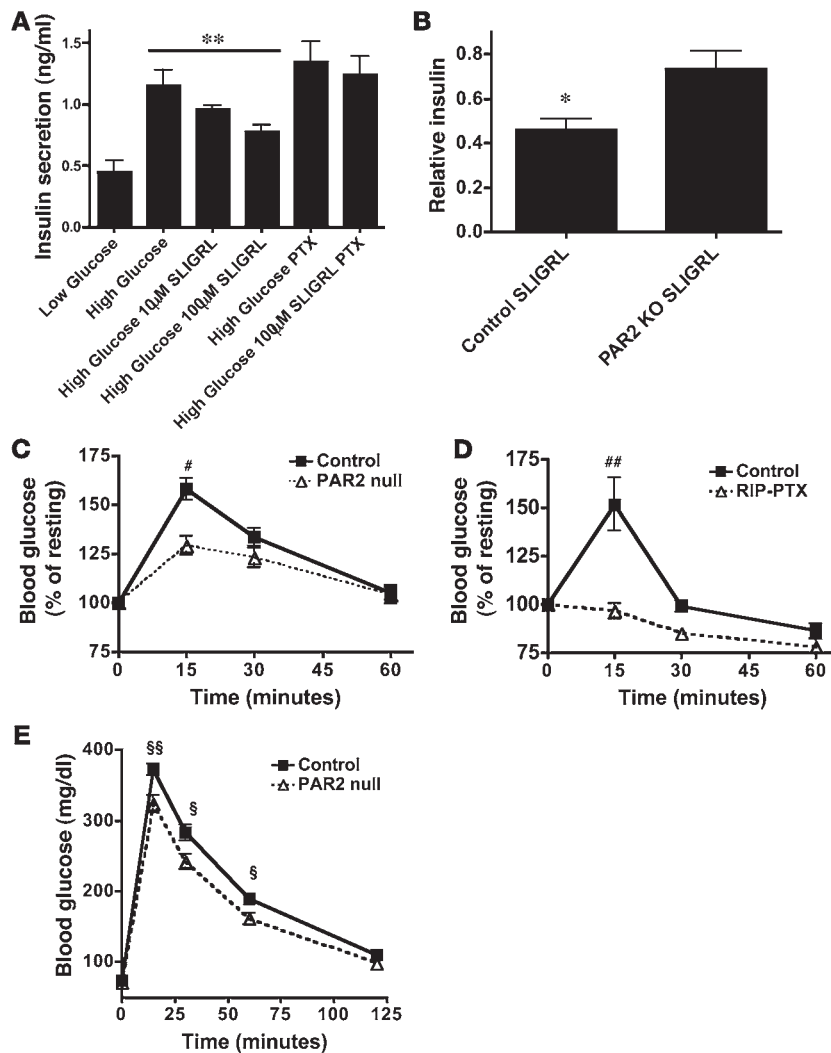
Figure 6
Par2 inhibits insulin release in vitro and in vivo. (**A**) Insulin levels in conditioned medium from β cell–like MIN6 cells. Cells were incubated in low (3 mM) or high (15 mM) glucose in the presence or absence of the Par2 agonist SLIGRL. SLIGRL (100 μM) inhibited GSIS ($n = 4$; **$P = 0.0055$, control versus 100 μM), and this was prevented by pretreatment with pertussis toxin (50 ng/ml for 16 hours). (**B**) Plasma insulin levels were measured at time 0 and again at 3 minutes following administration of vehicle or SLIGRL (10 μmol/kg, i.p.). Note the larger SLIGRL-induced decrease in plasma insulin levels in control relative to $Par2^{-/-}$ mice ($n = 12$; *$P = 0.012$). (**C**) $Par2^{-/-}$ and littermate control mice were fasted for 2 hours then dosed with SLIGRL (10 μmol/kg, i.p.); blood glucose levels were measured at the indicated times after SLIGRL administration. Data are expressed relative to glucose levels at time 0 for each genotype (123 ± 10 mg/dl, control; 118 ± 13 mg/dl, $Par2^{-/-}$). Littermate control mice became hyperglycemic relative to $Par2^{-/-}$ mice ($n = 12–13$; **$P < 0.01$). (**D**) RIP-PTX and littermate control mice were treated as in **C**. Basal glucose levels were 124 ± 14 mg/dl in littermate control mice and 86 ± 13 mg/dl in RIP-PTX mice. RIP-PTX mice failed to show glucose elevations in response to SLIGRL ($n = 7–9$; **$P < 0.001$). (**E**) Blood glucose levels in $Par2^{-/-}$ and littermate controls after i.p. glucose administration (IPGTT). Increases in blood glucose levels were blunted in $Par2^{-/-}$ mice compared with controls ($n = 29–35$; $P = 0.0006$ for difference between genotypes, 2-way ANOVA; **$P = 0.001$, *$P = 0.01$, difference in glucose levels at individual time points, unpaired Student's t test).

Par2 inhibits insulin release in a PTX-sensitive manner. Par2 mRNA was enriched in mouse and human islets compared with mixed tissue samples and was readily detected in 2 β cell lines (Figure 4 and Supplemental Figure 6). SLIGRL, a Par2 peptide agonist (34), inhibited GSIS in the MIN6 β cell line in a concentration-dependent and PTX-sensitive manner (Figure 6A). Administration of SLIGRL to wild-type mice caused a rapid decrease in blood insulin to less than half of normal levels; in *Par2*-null mice, SLIGRL administration caused only an approximately 20% decrease in blood insulin levels (Figure 6B). Similarly, SLIGRL injection led to a 50%–60% increase in blood glucose levels in wild-type mice within 15 minutes, and such increases were attenuated or completely abrogated in *Par2*-null and RIP-PTX mice, respectively (Figure 6, C and D). The effect of SLIGRL injection on glucose and insulin levels in *Par2*-null mice was indistinguishable from the effect of vehicle and may be mediated by adrenergic receptor activated by the sympathetic nervous system upon handling of conscious mice. The absence of SLIGRL effects in RIP-PTX mice is consistent with this explanation. Taken together, these findings suggest that activation of Par2 in β cells can inhibit insulin release via a $G_{i/o}$-dependent mechanism.

To assess the physiological importance of Par2 in glucose homeostasis in vivo, we performed an IPGTT in *Par2*-null mice and littermate

controls. *Par2*-null mice showed a subtle improvement in glucose tolerance compared with littermate controls ($n = 29–35$; $P = 0.0006$ by 2-way ANOVA) (Figure 6E). While the effect of Par2 deficiency was modest (peak glucose levels after i.p. glucose were 370 in controls and 320 in *Par2*-nulls), these data suggest that Par2 and hence protease signaling may play a previously unsuspected role in the physiological regulation of insulin secretion and glucose homeostasis.

Discussion
Conditional expression of diphtheria toxin fragment A from the *ROSA26* locus has been used for lineage ablation studies in mouse (35), and a transgenic mouse that constitutively expressed PTX in T cells has been used to assess the role of $G_{i/o}$ in that cell type (36). Our results indicate that conditional expression of PTX S1 subunit via the $ROSA26^{PTX}$ allele can be used to inhibit $G_{i/o}$ signaling in a cell type–specific manner that yields phenotypes not previously detected in individual $G_{i/o}$ knockouts. Given the panoply of Cre transgenes available, the $ROSA26^{PTX}$ allele provides a versatile new system for studying $G_{i/o}$ signaling in vivo. The cell type specificity of the $ROSA26^{PTX}$ conditional system permits detection of novel phenotypes masked by the more severe phenotypes in global $G_{i/o}$ family knockouts (5), and the ability of PTX to inhibit multiple members

of the $G_{i/o}$ family may reveal new phenotypes by overcoming redundancy. Because the switched-on $ROSA26^{PTX}$ allele is dominant, a single cross of a $ROSA26^{PTX/PTX}$ mouse to a Cre-transgenic mouse provides offspring that lack $G_{i/o}$ signaling in the lineage of interest, and studies can be done in a G_z-knockout background to further ablate G_i signaling with still-practical breeding schemes.

The fact that both RIP-Cre $Tg^{+/o}$:$ROSA26^{PTX/+}$ and PDX-Cre $Tg^{+/o}$:$ROSA26^{PTX/+}$ mice had normal pancreas development, structurally normal islets, and a persistent gain-of-function phenotype (increased insulin secretion) emphasizes that chronic expression of PTX S1 from the $ROSA26$ locus did not negatively affect β cell health and did yield a cell type– and $G_{i/o}$-specific phenotype. In addition to supporting use of the $ROSA26^{PTX}$ mouse to probe for roles of $G_{i/o}$ signaling in other cell lineages and processes, this result supports exploration of conditional expression of other protein "toxins" that specifically alter intracellular signaling pathways.

The peak insulin level achieved after glucose administration to RIP-PTX mice was approximately 15-fold higher than that achieved in wild-type mice. With appropriate caveats regarding comparisons across studies, this increase appears to be greater than that reported in knockouts of single GPCRs known to negatively regulate insulin secretion (20–22). These observations and the resistance of these mice to diet-induced diabetes emphasizes a key role for G_i signaling in β cells in modulating moment-to-moment insulin secretion and glucose homeostasis and are consistent with the notion that β cells integrate inputs from multiple $G_{i/o}$-coupled GPCRs that negatively modulate insulin secretion.

Quantitation of GPCR mRNA expression in islets by qRT-PCR proved useful for identifying candidate receptors that might regulate insulin secretion. mRNAs for receptors such as glucagon-like peptide 1 receptor and GPR40, which are known to regulate β cell insulin secretion (37, 38), were among those most highly and specifically expressed in islets, but mRNAs for receptors not previously suspected of regulating insulin secretion were also found at high levels (Figure 4). The study of one such receptor, Taar1, led to the finding that its recently described ligand, the thyroid hormone metabolite T1AM, can regulate insulin release. In addition, we found that, like other biogenic amines, T1AM can activate several GPCRs (Taar1 and Adra2a receptor) to activate predominantly G_s or G_i signaling depending on relative expression levels of its receptors.

The affinity of T1AM for Adra2a was in the micromolar range (Figure 5F), an affinity equal to or greater than that of the classic endogenous adrenergic receptor agonist epinephrine. However, the concentrations of T1AM measured in the circulation thus far have been in the nanomolar range (T.S. Scanlan, unpublished observations), and whether circulating T1AM ever reaches a level sufficient to activate Adra2a in vivo is unknown. Similarly, the enzymes predicted to generate T1AM from thyroid hormones are expressed in pancreatic islets (ref. 39 and our unpublished observations), but whether local synthesis, storage, and release can indeed increase local T1AM concentration remains to be determined. TAAR1 and ADRA2A are expressed in human islets (Supplemental Figure 6) (40), and regardless of whether T1AM is a physiological stimulator of insulin release via Taar1 or an inhibitor of insulin release via Adra2a, our results support the notion that pharmacological agonism of Taar1 and/or antagonism of Adra2a might be explored to augment insulin secretion for therapeutic purposes.

The ability of Par2 agonists to inhibit insulin release in a β cell $G_{i/o}$–dependent manner and the improved clearance of blood glucose in $Par2$-null mice, however modest, suggest that Par2 may be a physiological regulator of β cell function. While serine proteases regulate insulin secretion indirectly through the production and degradation of peptide secretagogues (41), direct regulation of β cell insulin release by a protease has not, to our knowledge, been previously described. Exactly what β cell Par2 senses biochemically and physiologically remains to be determined. The exocrine pancreas surrounding the islets is an abundant source of trypsin, which can activate Par2. Thus, it is conceivable that activation of β cell Par2 represents a pathway for crosstalk between the exocrine and endocrine pancreas. More plausibly, other proteases produced and/or activated locally within the islet itself might be the relevant activators. While the improvement in glucose tolerance in Par2-deficient mice compared with their control littermates was not large, it appears to become larger with age (data not shown). Whether Par2 regulation of insulin secretion might become more important under physiological stresses, such as high-fat diet, remains to be determined.

The list of GPCRs highly and specifically expressed in islets (Figure 4 and Table 1) reveals other interesting candidate regulators of insulin secretion. Included in these are GPRC6A, among the most islet-specific in our studies, and GPR41 and GPR43, among the most abundant. We confirmed that these receptors are expressed in human and mouse islets and in 2 β cell lines (J.B. Regard and S.R. Coughlin, unpublished observations). GPRC6A may be activated by arginine and lysine (42), basic amino acids that can stimulate β cell insulin secretion (43), by a mechanism as yet incompletely understood. Might insulin secretion in response to basic amino acids be mediated by GPRC6A? Similarly, GPR41 and GPR43 were recently shown to be receptors for short-chain fatty acids (44). Their relative, GPR40, also highly expressed in islets (Figure 4 and ref. 37), triggers insulin secretion in β cell lines in response to longer-chain fatty acids. Short-chain fatty acids constitute approximately 5%–10% of dietary energy supply in nonruminants (45). Might GPR41 or GPR43 mediate insulin secretion in response to dietary short-chain fatty acids? Our results should stimulate investigation of the roles of these and other GPCRs as potential regulators of β cell function and glucose homeostasis. More broadly, the $ROSA26^{PTX}$ mouse and quantitative GPCR expression profiling provide a system that should be useful for uncovering new roles for GPCRs in other cell lineages and physiological processes.

Methods

Generation of $ROSA26^{PTX}$ mice. Mouse care and use for these studies was approved by the UCSF Institutional Animal Care and Use Committee. The $ROSA26^{PTX}$ targeting vector was generated using pROSA26-1, pSAβgeo, and pPGK-neo-tpA-2loxP plasmids (46) (gifts from Philippe Soriano, University of Washington, Seattle, Washington, USA). The XbaI site of the pROSA26-1 plasmid, containing $ROSA26$ genomic sequences and a PGK–diphtheria toxin cassette, was modified to contain PacI and AscI sites. The β-geo sequence of pSAβgeo was replaced by the loxP-PGK-neo-tpA-loxP cassette from pPGK-neo-tpA-2loxP. In the resulting pSAfloxPGK-neotpA plasmid, a PacI site and XhoI-SwaI-NotI-AscI sites were created 5′ to the splice acceptor (SA) and 3′ to the lox-P-PGK-neo-tpA-loxP cassette, respectively (pSAfloxPGK-neotpA2). PTX S1 cDNA (a gift from Eitan Reuveny, Weizmann Institute of Science, Rehovot, Israel) was first cloned into pBS-SK+, and a silent mutation was introduced to destroy the SalI site. This PTX S1 with a C-terminal myc tag was ligated to the rabbit globin poly(A) sequence and subcloned into the XhoI-NotI sites of the pSAfloxPGK-neotpA2. The resulting pSAfloxPGK-neotpA2-PTX-pA was cloned into the PacI-AscI site of pROSA26-1 to generate the targeting vector, pROSA26-floxPGK-neot-

pA2-PTX, which was linearized using KpnI and electroporated into E14 ES cells. Following neomycin selection correct targeting was confirmed by Southern blot analyses using the 5′ *ROSA26* probe (a gift from P. Soriano), PTX transgene, and *ROSA26* coding region exon2 probes. ES cells (clone 7) were injected into blastocysts to generate chimeras that were in turn mated to C57BL/6 mice to obtain germline transmission of the *ROSA26^PTX* allele. All mice used were in a mixed C57BL/6/129SvJ background.

Other mice. CMV-IE-ERCre (13), RIP-Cre (16), PDX-Cre (19), *Adra2a*-null (47), and *Par2*-null (48) mice have been described previously.

ADP-ribosylation of embryonic fibroblast membrane fraction. ADP-ribosylation assays have been described previously (49). PTX holoenzyme was purchased from Calbiochem.

Immunohistochemistry. Immunohistochemistry was performed as described previously (50).

Blood glucose and insulin measurements. Blood glucose levels were measured using a portable glucometer (Therasense FreeStyle). Insulin levels in plasma and from cultured cells were quantified by ELISA (Mercodia Ultrasensitive Mouse Insulin ELISA). For relative insulin measurements, samples were collected at time 0 and again at the indicated time. Percent change in insulin was computed relative to time 0. IPGTT (2 g/kg glucose) and in vivo GSIS (3 g/kg glucose) tests were performed on mice following an overnight fast. For diet-induced diabetes studies, mice were fed high-fat diet (45% fat; TD.06415; Harlan Teklad) for 30 weeks.

Generation and validation of GPCR qRT-PCR array and real-time qPCR. cDNA sequences were compiled for mouse nonodorant GPCRs using the National Center for Biotechnology Information (http://www.ncbi.nlm.nih.gov/), International Union of Basic and Clinical Pharmacology (http://www.iuphar-db.org/), and G Protein–Coupled Receptor Data Base (http://www.gpcr.org/) databases and published work by others (23). Gene-specific TaqMan primer/probe sets (5′FAM/3′BHQ) for real-time PCR were designed for each GPCR using Primer Express software (Applied Biosystems) and were purchased from Biosearch Technologies. Of the primer-probe sets employed, 352 amplified products from at least one RNA source (whether the 21 GPCRs not amplified are expressed only in cell types not examined or represent pseudogenes or a failure of the specific primer-probe sets used is not known). Total RNA was isolated from tissues of interest first by TRIZOL (Invitrogen) extraction followed by purification with RNeasy Mini Column (QIAGEN). Genomic DNA contamination was avoided by DNaseI treatment (QIAGEN) of the RNA on the RNeasy column. First-strand cDNA synthesis was performed using the Superscript First-Strand Synthesis System (Invitrogen) and oligo-dT primers. Real-time PCR reactions were performed in a 384-well format using Platinum qPCR mix (Invitrogen) and total reaction volumes of 10 μl. Raw cycle threshold (Ct) data from ABI 7900HT (Applied Biosystems) was obtained with a fluorescence threshold of 0.2 for all reactions. In the absence of reverse transcription, the same RNA preparations gave no qRT-PCR signal for any of the GPCRs assayed. GPCR Ct data was normalized to a control for mRNA sample size using the ΔCt method and converted to fold-increase over abundance of each GPCR mRNA in mixed tissues using the ΔΔCt method. The mixed tissue sample included brain, spleen, thymus, kidney, bone marrow, and skeletal muscle. Control Ct values were calculated by averaging 3 control Ct values together (GAPDH, β-actin, cyclophilin). Dilution studies revealed that the amount of qRT-PCR product was directly proportional to the amount of starting material. TA cloning (Invitrogen) and sequencing of 12% of qPCR amplicons showed all to be the expected products.

Membrane binding experiments. Membrane binding was performed as described previously (51) on transiently transfected Cos7 cells using [³H]RX821002 (50 Ci/mmol; Amersham Biosciences). Equilibrium dissociation constants were determined from saturation isotherms and competition curves. Data were analyzed using Prism4 (GraphPad Software). All binding was transfection dependent.

In vitro GSIS. MIN6 cells were grown in DMEM (25 mM glucose), 2 mM glutamine, 15% FBS, 100 U/ml penicillin, 100 μg/ml streptomycin, 70 μM 2-mercaptoethanol. MIN6 cells were split 100,000 cells per well in 24-well plates. The following day, cells were switched to DMEM low-glucose (5.5 mM) medium and allowed to equilibrate overnight. On the third day, cells were washed with Krebs-Ringer-HEPES (KRH) buffer (115 mM NaCl, 4.7 mM KCl, 1.2 mM KH₂PO₄, 10 mM NaHCO₃, 1.28 mM CaCl₂, 1.2 mM MgSO₄, 10 mM HEPES [pH 7.4]) and preincubated in KRH with 0.1 mM glucose for 2 hours. Following preincubation, KRH containing the indicated reagents was added to the cells and incubated at 37°C for 30 minutes. Human and mouse islets were isolated by the UCSF islet isolation core and cultured 12–24 hours in nonadherent culture dishes using RPMI 1640 medium supplemented with 10% FBS, antibiotics, and 5 mM glucose. Six to 10 islets were handpicked into modified Krebs-Ringer bicarbonate buffer (KRBB) containing 2.8 mM glucose and cultured for 1 hour at 37°C. Islets were incubated for 30 minutes in 2.8 and 17.8 mM glucose KRBB with T1AM or vehicle. Supernatants were collected to quantify secreted insulin; islets were collected to quantify total insulin. T1AM was used at 10 μM; PTX treatment (50 ng/ml) was done overnight during equilibration step. Supernatants were collected and analyzed for insulin content by ELISA (Mercodia).

Statistics. Two-way ANOVA with Bonferroni post-tests and unpaired 2-tailed Student's *t* test were used where appropriate. Graphical data are shown as mean ± SEM unless otherwise specified. $P < 0.05$ was considered significant.

Address correspondence to: Shaun R. Coughlin, University of California, San Francisco, 600 16th Street, Room S472D, San Francisco, California 94143-2240, USA. Phone: (415) 476-6174; Fax: (415) 476-8173; E-mail: Shaun.Coughlin@ucsf.edu.

Thomas S. Scanlan's present address is: Oregon Health & Science University, Portland, Oregon, USA.

Jean B. Regard and Hiroshi Kataoka contributed equally to this work.

1. Hopkins, A.L., and Groom, C.R. 2002. The druggable genome. *Nat. Rev. Drug Discov.* **1**:727–730.
2. Civelli, O. 2005. GPCR deorphanizations: the novel, the known and the unexpected transmitters. *Trends Pharmacol. Sci.* **26**:15–19.
3. Offermanns, S., Mancino, V., Revel, J.P., and Simon, M.I. 1997. Vascular system defects and impaired cell chemokinesis as a result of Galpha13 deficiency. *Science.* **275**:533–536.
4. Offermanns, S., Toombs, C.F., Hu, Y.H., and Simon, M.I. 1997. Defective platelet activation in G alpha(q)-deficient mice. *Nature.* **389**:183–186.
5. Rudolph, U., et al. 1995. Ulcerative colitis and adenocarcinoma of the colon in G alpha i2-deficient mice. *Nat. Genet.* **10**:143–150.
6. Yu, S., et al. 1998. Variable and tissue-specific hormone resistance in heterotrimeric Gs protein alpha-subunit (Gsalpha) knockout mice is due to tissue-specific imprinting of the gsalpha gene. *Proc. Natl. Acad. Sci. U. S. A.* **95**:8715–8720.
7. Gierschik, P. 1992. ADP-ribosylation of signal-

transducing guanine nucleotide-binding proteins by pertussis toxin. *Curr. Top. Microbiol. Immunol.* **175**:69–96.

8. Gulbenkian, A., Schobert, L., Nixon, and Tabachnick, I.I. 1968. Metabolic effects of pertussis sensitization in mice and rats. *Endocrinology.* **83**:885–892.

9. Tabachnick, I.I., and Gulbenkian, A. 1969. Adrenergic changes due to pertussis: insulin, glucose and free fatty acids. *Eur. J. Pharmacol.* **7**:186–195.

10. Katada, T., and Ui, M. 1979. Islet-activating protein. Enhanced insulin secretion and cyclic AMP accumulation in pancreatic islets due to activation of native calcium ionophores. *J. Biol. Chem.* **254**:469–479.

11. Katada, T., and Ui, M. 1981. In vitro effects of islet-activating protein on cultured rat pancreatic islets. Enhancement of insulin secretion, adenosine 3′:5′-monophosphate accumulation and 45Ca flux. *J. Biochem. (Tokyo).* **89**:979–990.

12. Soriano, P. 1999. Generalized lacZ expression with the ROSA26 Cre reporter strain. *Nat. Genet.* **21**:70–71.

13. Hayashi, S., and McMahon, A.P. 2002. Efficient recombination in diverse tissues by a tamoxifen-inducible form of Cre: a tool for temporally regulated gene activation/inactivation in the mouse. *Dev. Biol.* **244**:305–318.

14. Tamura, M., et al. 1982. Subunit structure of islet-activating protein, pertussis toxin, in conformity with the A-B model. *Biochemistry.* **21**:5516–5522.

15. Postic, C., et al. 1999. Dual roles for glucokinase in glucose homeostasis as determined by liver and pancreatic beta cell-specific gene knock-outs using Cre recombinase. *J. Biol. Chem.* **274**:305–315.

16. Gannon, M., et al. 2000. Analysis of the Cre-mediated recombination driven by rat insulin promoter in embryonic and adult mouse pancreas. *Genesis.* **26**:139–142.

17. Lee, J.Y., et al. 2006. RIP-Cre revisited, evidence for impairments of pancreatic beta-cell function. *J. Biol. Chem.* **281**:2649–2653.

18. Lin, X., et al. 2004. Dysregulation of insulin receptor substrate 2 in beta cells and brain causes obesity and diabetes. *J. Clin. Invest.* **114**:908–916. doi:10.1172/JCI200422217.

19. Gannon, M., Herrera, P.L., and Wright, C.V. 2000. Mosaic Cre-mediated recombination in pancreas using the pdx-1 enhancer/promoter. *Genesis.* **26**:143–144.

20. Fagerholm, V., et al. 2004. Altered glucose homeostasis in alpha2A-adrenoceptor knockout mice. *Eur. J. Pharmacol.* **505**:243–252.

21. Pedrazzini, T., et al. 1998. Cardiovascular response, feeding behavior and locomotor activity in mice lacking the NPY Y1 receptor. *Nat. Med.* **4**:722–726.

22. Wang, X.P., et al. 2004. Double-gene ablation of SSTR1 and SSTR5 results in hyperinsulinemia and improved glucose tolerance in mice. *Surgery.* **136**:585–592.

23. Vassilatis, D.K., et al. 2003. The G protein-coupled receptor repertoires of human and mouse. *Proc. Natl. Acad. Sci. U. S. A.* **100**:4903–4908.

24. Jensen, S.L., Holst, J.J., Nielsen, O.V., and Lauritsen, K.B. 1981. Secretory effects of gastric inhibitory polypeptide on the isolated perfused porcine pancreas. *Acta. Physiol. Scand.* **111**:233–238.

25. Fehmann, H.C., et al. 1989. Synergistic stimulatory effect of glucagon-like peptide-1 (7-36) amide and glucose-dependent insulin-releasing polypeptide on the endocrine rat pancreas. *FEBS Lett.* **252**:109–112.

26. Leblanc, H., Anderson, J.R., Sigel, M.B., and Yen, S.S. 1975. Inhibitory action of somatostatin on pancreatic alpha and beta cell function. *J. Clin. Endocrinol. Metab.* **40**:568–572.

27. Hramiak, I.M., Dupre, J., and McDonald, T.J. 1988. Effects of galanin on insulin responses to hormonal, neuropeptidal, and pharmacological stimuli in conscious dogs. *Endocrinology.* **122**:2486–2491.

28. Borowsky, B., et al. 2001. Trace amines: identification of a family of mammalian G protein-coupled receptors. *Proc. Natl. Acad. Sci. U. S. A.* **98**:8966–8971.

29. Bunzow, J.R., et al. 2001. Amphetamine, 3,4-methylenedioxymethamphetamine, lysergic acid diethylamide, and metabolites of the catecholamine neurotransmitters are agonists of a rat trace amine receptor. *Mol. Pharmacol.* **60**:1181–1188.

30. Coughlin, S.R. 1999. How the protease thrombin talks to cells. *Proc. Natl. Acad. Sci. U. S. A.* **96**:11023–11027.

31. Scanlan, T.S., et al. 2004. 3-Iodothyronamine is an endogenous and rapid-acting derivative of thyroid hormone. *Nat. Med.* **10**:638–642.

32. Gromada, J., et al. 2004. ATP-sensitive K+ channel-dependent regulation of glucagon release and electrical activity by glucose in wild-type and SUR1-/- mouse alpha-cells. *Diabetes.* **53**(Suppl. 3):S181–S189.

33. Bylund, D.B. 1988. Subtypes of alpha 2-adrenoceptors: pharmacological and molecular biological evidence converge. *Trends Pharmacol. Sci.* **9**:356–361.

34. Lerner, D.J., Chen, M., Tram, T., and Coughlin, S.R. 1996. Agonist recognition by proteinase-activated receptor 2 and thrombin receptor. Importance of extracellular loop interactions for receptor function. *J. Biol. Chem.* **271**:13943–13947.

35. Brockschnieder, D., et al. 2004. Cell depletion due to diphtheria toxin fragment A after Cre-mediated recombination. *Mol. Cell. Biol.* **24**:7636–7642.

36. Chaffin, K.E., et al. 1990. Dissection of thymocyte signaling pathways by in vivo expression of pertussis toxin ADP-ribosyltransferase. *EMBO J.* **9**:3821–3829.

37. Itoh, Y., et al. 2003. Free fatty acids regulate insulin secretion from pancreatic beta cells through GPR40. *Nature.* **422**:173–176.

38. Thorens, B. 1992. Expression cloning of the pancreatic beta cell receptor for the gluco-incretin hormone glucagon-like peptide 1. *Proc. Natl. Acad. Sci. U. S. A.* **89**:8641–8645.

39. Lindstrom, P. 1986. Aromatic-L-amino-acid decarboxylase activity in mouse pancreatic islets. *Biochim. Biophys. Acta.* **884**:276–281.

40. Lacey, R.J., et al. 1996. Expression of alpha 2- and beta-adrenoceptor subtypes in human islets of Langerhans. *J. Endocrinol.* **148**:531–543.

41. Holst, J.J., and Deacon, C.F. 1998. Inhibition of the activity of dipeptidyl-peptidase IV as a treatment for type 2 diabetes. *Diabetes.* **47**:1663–1670.

42. Wellendorph, P., et al. 2005. Deorphanization of GPRC6A: a promiscuous L-alpha-amino acid receptor with preference for basic amino acids. *Mol. Pharmacol.* **67**:589–597.

43. Jarrousse, C., and Rosselin, G. 1975. Interaction of amino acids and cyclic AMP on the release of insulin and glucagon by newborn rat pancreas. *Endocrinology.* **96**:168–177.

44. Brown, A.J., et al. 2003. The Orphan G protein-coupled receptors GPR41 and GPR43 are activated by propionate and other short chain carboxylic acids. *J. Biol. Chem.* **278**:11312–11319.

45. Bergman, E.N. 1990. Energy contributions of volatile fatty acids from the gastrointestinal tract in various species. *Physiol. Rev.* **70**:567–590.

46. Srinivas, S., et al. 2001. Cre reporter strains produced by targeted insertion of EYFP and ECFP into the ROSA26 locus. *BMC Dev. Biol.* **1**:4.

47. Altman, J.D., et al. 1999. Abnormal regulation of the sympathetic nervous system in alpha2A-adrenergic receptor knockout mice. *Mol. Pharmacol.* **56**:154–161.

48. Camerer, E., Kataoka, H., Kahn, M., Lease, K., and Coughlin, S.R. 2002. Genetic evidence that protease-activated receptors mediate factor Xa signaling in endothelial cells. *J. Biol. Chem.* **277**:16081–16087.

49. Hung, D.T., Vu, T.H., Nelken, N.A., and Coughlin, S.R. 1992. Thrombin-induced events in non-platelet cells are mediated by the unique proteolytic mechanism established for the cloned platelet thrombin receptor. *J. Cell Biol.* **116**:827–832.

50. Hebrok, M., Kim, S.K., St. Jacques, B., McMahon, A.P., and Melton, D.A. 2000. Regulation of pancreas development by hedgehog signaling. *Development.* **127**:4905–4913.

51. Link, R., Daunt, D., Barsh, G., Chruscinski, A., and Kobilka, B. 1992. Cloning of two mouse genes encoding alpha 2-adrenergic receptor subtypes and identification of a single amino acid in the mouse alpha 2-C10 homolog responsible for an interspecies variation in antagonist binding. *Mol. Pharmacol.* **42**:16–27.